

# Molecular Mobility in Starchy Materials Studied by Electron Spin Resonance

Anne-Marie Riquet,<sup>1</sup> Alexandra Feigenbaum,<sup>1</sup> Paul Colonna,<sup>2</sup> Denis Lourdin<sup>2</sup>

<sup>1</sup>INRA-Laboratoire de Nutrition et Sécurité Alimentaire, Domaine de Vilvert, 78350 Jouy en Josas, France

<sup>2</sup>INRA-Unité de Recherche sur les Polysaccharides Leurs Organisations et Interactions BP 71627, 44316 Nantes Cedex, France

Received 9 January 2002; accepted 14 May 2002

**ABSTRACT:** Phase transitions in hydrated starch–sorbitol system were investigated both by molecular (electron spin resonance, ESR) and macroscopic (differential scanning calorimetry, DSC) methods. In rapid-tumbling region, one did not observe the same phenomena by DSC and by ESR. The transitions observed by ESR, which seemed to reflect more the interactions probe–matrix than plasticization, probably corresponded to the interactions probe–sorbitol. For system concentrated in plasticizer, it was conceivable to admit that

a demixion of sorbitol occurred. In slow-tumbling region, a correspondence in temperature mobility changes measured by mechanical spectroscopy and ESR was observed. © 2003 Wiley Periodicals, Inc. *J Appl Polym Sci* 88: 990–997, 2003

**Key words:** starch; sorbitol; phase separation; molecular mobility; electron spin resonance; differential scanning calorimetry

## INTRODUCTION

During the last years, there has been an increasing interest in systems containing starch in the amorphous state, usually in low moisture systems, as they have widespread industrial uses. It can also be envisaged that amorphous starch, as a material, has good barrier properties, and that it could replace ethylene-vinyl alcohol copolymer (EVOH), another polar polymer, in multilayer structures.

Generally, these systems in food or nonfood applications contain low-molecular-weight components like sugar, which greatly modify their properties. Macroscopic properties and particularly mechanical properties of polymeric system are usually interpreted in terms of polymer chain mobility. Above  $T_g$ , important molecular mobility leads to suppleness and deformable properties of the material. In glassy state, below  $T_g$ , the viscosity of the polymer is extremely high, the material is rigid and brittle due to reduced chain mobility. Only localized molecular mobility evidenced by mechanical or dielectric dynamic method is observed. In order to process starch into multilayers, it is important to be able to adjust both the glass transition of the material and the viscosity of starch by addition of glycerol or sorbitol as plasticizers.

The phase and state behavior of similar systems composed of starch, water and a low-molecular-

weight carbohydrate have been studied previously and the interpretation of results is still subject to debate.<sup>1</sup> A phase-separated system that contains polymer-rich (starch) and plasticizer-rich (low-molecular-weight carbohydrate) domains is suspected. In this case, the system reveals two glass transition, at high- and low-temperature domain. All these observations are complicated by the evolution of the phases with time, during the preparation and the storage of samples. However, this can also affect the permeability of the material, as well as its homogeneity. Previous works have shown the relation between these mechanical properties, diffusion and stability with molecular mobility on the ternary system starch–sorbitol–water.<sup>2,3</sup> For this reason, this study was realized on the same system. It is the purpose of this work to investigate phase transitions and separation in hydrated starch–sorbitol materials by molecular (electron spin resonance, ESR) and macroscopic investigation methods (differential scanning calorimetry DSC). The sorbitol, potentially crystalline, is a representative plasticizer or sugar.

## EXPERIMENTAL

### Sample preparation

Starch films were obtained by the casting method. Native wheat starch (Amylum, France) was solubilized in a high-pressure reactor at 130°C for 20 min using a 4% suspension in ultrapure water with precise quantities of sorbitol. The experiments were conducted under a nitrogen atmosphere to avoid any degradation. After cooling at 80°C, a probe (5,000 mg

Correspondence to: Anne-Marie Riquet (riquet@ensia.inra.fr).  
Contract grant sponsor: Ademe in Agrice project.

TABLE I  
Composition of Various Samples Studied

DSC		ESR (TEMPOL)		ESR (DMAT)		Nomenclature
Starch/sorbitol	% water (d.b.)	Starch/sorbitol	% water (d.b.)	Starch/sorbitol	% water (d.b.)	
100/0	13.8	100/0	13.9	100/0	13.9	0
		94/6	9.9	95/5	9.9	5
89/11	10.0	89/11	9.9	92/8	9.9	10
				83/17	10.5	17
		74/26	10.5	74/26	10.5	26
71/29	11.1			71/29	11.1	30
		60/40	12.3	60/40	12.3	40
0/100	12.3	0/100	12.3	0/100	12.3	100

Water contents are expressed in per 100 of dry basis (d.b.) constituted by starch and sorbitol.

per kg dry starch) was added. Each sample contained only one probe. The solution was evenly spread on a Teflon-coated hot plate maintained at 70°C, until the film no longer adhered to the plate and edge curling occurred. The transparent film obtained contained about 10% water (dry basis). Films were stored for 48 h in an atmosphere controlled by a saturated sodium bromide solution (RH 57% at 25°C). Films were reduced to a powder using a cryogrinder.

Table I lists the composition of samples prepared for DSC and ESR measurements. The water content determined by thermogravimetric analysis results in the conditioning at the equilibrium relative humidity of 57%. It is expressed in percent per dry basis containing starch and sorbitol in various proportion. In order to simplify the text, samples will be sometimes identified by the proportion of sorbitol in the dry basis.

### DSC measurements

DSC measurements were performed on automated DSC 121 equipment (SETARAM, France). The DSC was calibrated for temperature from the melting points of indium (156.6°C) and gallium (29.8°C). Powders were placed in pressure-tight DSC cells (about 80 mg of matter per cell). The calorimetric measurement procedure was similar for all samples regardless of composition. A first scanning was performed from -48 to 125°C to observe the influence of aging during the storage of the samples. Rapid cooling (60°C/min) to -48°C allowed the starch-sorbitol system to be frozen in an amorphous state. A second scanning was performed at 3°C/min.

### Spin probes

Three spin probes having different functional groups were selected (Fig. 1): 2,2,6,6-tetramethylpiperidin-1-oxyl (TEMPO), and 4-hydroxy-2,2,6,6-tetramethylpiperidin-1-oxyl (4-hydroxy-TEMPO) (TEMPOL) were commercially available (Aldrich Chemical) and used without further purification; 4-dimethylamino-2,2,6,6-

tetramethylpiperidin-1-oxyl (4-dimethylamino-TEMPO) (DMAT) has been synthesized in high yield in the laboratory.<sup>4</sup>

### ESR measurements

The powder was introduced in a glass capillary (1.5 mm), which was immediately sealed. The sample height in the capillary tube was about 2 cm. Before analysis, the tube was heated to 120°C (10°C/min) and maintained at 120°C for 10 min to get rid of the thermal history of the sample (enthalpy relaxation). Rapid cooling (liquid N<sub>2</sub>) to -30°C allowed the starch-sorbitol system to be frozen in an amorphous state.

ESR spectra were measured with a Bruker ESP 300 spectrometer in the temperature range -80°C to 140°C. Samples (in glass capillaries) were placed in the ESR tube (d = 0.32 cm; h = 18 cm) and analyzed directly in the spectrometer cavity. The hyperfine split ( $2A'_{zz}$ ) of the spectrum was measured as the distance (in Gauss) between the two extreme peaks.

$T_{50G}$  has been defined experimentally<sup>5</sup> as the temperature at which  $2A'_{zz} = 50$  Gauss. Values of  $T_{50G}$  are obtained conveniently from plots of  $2A'_{zz}$  versus temperature, which are typically sigmoidal in shape.  $T_{50G}$  is the temperature at which the sigmoidal curves dis-

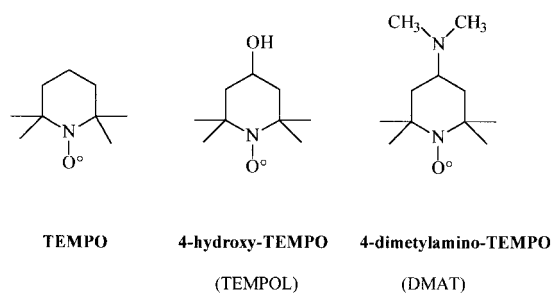
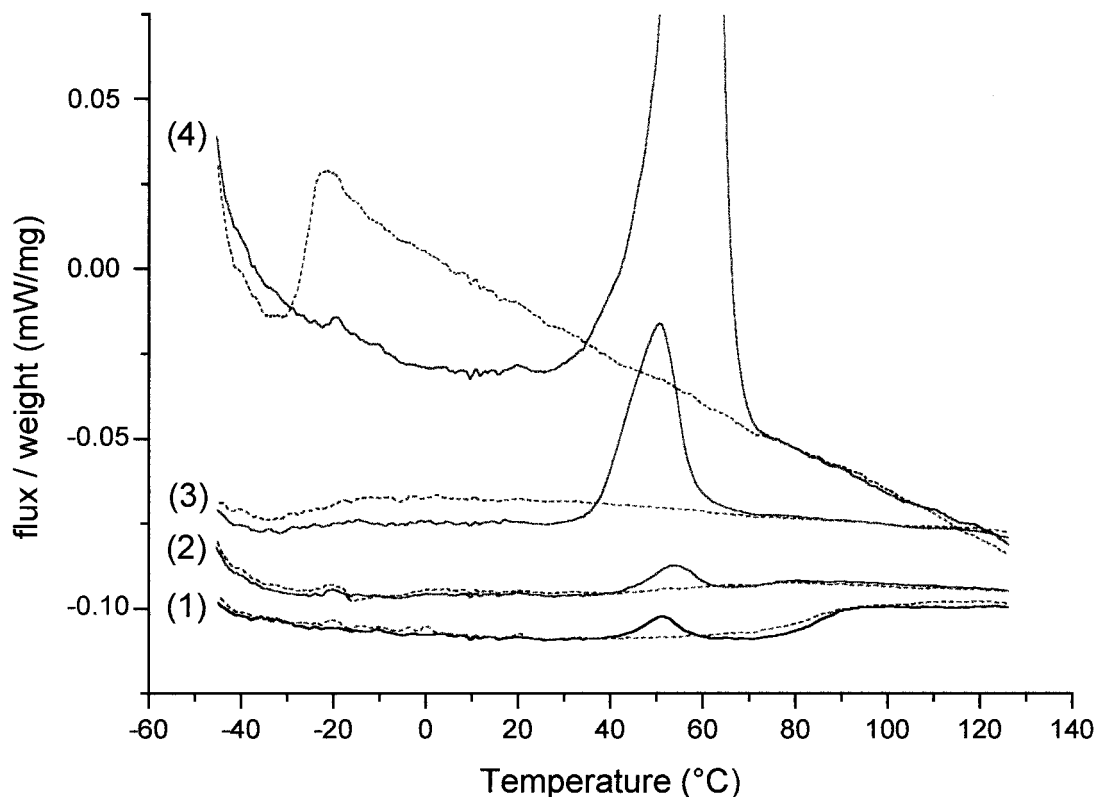


Figure 1 Chemical structure of the paramagnetic probes.



**Figure 2** Thermograms of starch-sorbitol 100/0 containing 13.8% water d.b. (1); 89/11, 10% (2); 71/29, 11.1% (3); 0/100, 12.3% (4). Dashed line: first scan; continuous line: second scan.

play a sharp break. The lower the  $T_{50G}$  is, the higher the mobility of the radical.

The approach of Kuznetsov and Ebert<sup>6</sup> was used to determine the rotational diffusion model for each of the probes in the slow-tumbling region, that is, below  $T_{50G}$  ( $5 \times 10^{-9} \leq \tau_r < 10^{-7}$  sec). In this approach, the change in position of the low-field [ $\Delta_{(+)}$ ] and high-field [ $\Delta_{(-)}$ ] peaks relative to their rigid limit positions is determined:

$$R = \Delta_{(-)}/\Delta_{(+)} \text{ vs. } \Delta_{(+)} \quad (1)$$

To estimate the rotational correlation time ( $\tau_r$ ) in the region of slow rotation, the following expression<sup>7</sup> is used:

$$\tau_r = a[1 - (2A'_{zz}/2A_{zz})]^b \quad (2)$$

where  $2A_{zz}$  is the peak-to-peak separation of the rigid limit spectrum (extreme separation),  $2A'_{zz}$  is the peak-to-peak separation at higher temperatures;  $a$  and  $b$  are values depending on line width and rotational diffusion models. According to a mean value of 3 Gauss for the line widths of the three probes in frozen starch,  $a = 5.4 \times 10^{-10}$  and  $b = 1.36$  for a Brownian rotational diffusion; and  $a = 1.1 \times 10^{-10}$  and  $b = 1.01$  for a free diffusion.

Assuming that the rotation of radicals is an activated process, the temperature dependence of  $\tau_r$  can be expressed by the Arrhenius equation:

$$\tau_r = \tau_o \exp(E_a/RT) \quad (3)$$

where  $\tau_o$  is the preexponential factor,  $E_a$  the effective activation energy,  $R$  the gas constant, and  $T$  the temperature (K).

## RESULTS AND DISCUSSION

### DSC

Typical DSC scans of hydrated starch-sorbitol mixtures are shown in Figure 2. The thermogram has been chosen as representative of the results obtained on all the concentration domain of the system, from hydrated starch to hydrated sorbitol. The first and second scan obtained for each sample are compared.

For thermogram obtained on amorphous starch hydrated to 13.8% water d.b., two events are clearly observed on the first scan. From lower temperatures, the first event is an endothermic peak appearing at 50–60°C on the first scan and vanishing on the second scan. It corresponds to the recovery of the enthalpy relaxed during structural relaxation occurring during

storage of the sample at temperature below  $T_g$ .<sup>8</sup> The structural relaxation occurs very slowly and gives rise to the phenomenon of physical aging, which is associated with a change in material properties.<sup>9</sup> Concerning the second event, the sharp change in heat capacity in the region of 80–90°C indicates the glass transition of the hydrated starch. The  $T_g$  determined at 90°C is according to results published by Bizot et al.<sup>10</sup> on glass transition of amorphous starch containing 13.8% d.b. of water.

Concerning hydrated sorbitol, the first scan reveals an intense endothermic peak whose maximum is situated at 58°C. According to published values on the sorbitol–water phase diagram,<sup>11</sup> this event corresponds to the fusion of crystalline sorbitol. On the second scan, the glass transition of the amorphous state of the vitrified sorbitol is observed at –25°C. If the sample is maintained at temperature above the glass transition, the nonequilibrium glassy state will progressively evolve to the more stable crystalline state. After a period of time at ambient temperature, the fusion of crystalline sorbitol at 58°C will be again observable.

Because enthalpy recovery of starch on the one hand and fusion of sorbitol on the other hand appear in the same temperature domain, results obtained on intermediate composition are not clear-cut. The thermograms of the sample containing 11% sorbitol are close to those obtained for hydrated starch with the peak at 50–60°C due to structural relaxation, which could contain a part attributed to sorbitol fusion. Inversely for the sample containing 29% sorbitol, its behavior is close to hydrated sorbitol with the fusion of sorbitol at 50–60°C, which could contain a part of enthalpy recovery. The observation of a peak of fusion in mixtures, close to the temperature of the fusion of hydrated sorbitol, confirms the phase-separated sorbitol evoked previously.<sup>12</sup> The glass transition of the hydrated starch–sorbitol system, which has been measured in a previous work<sup>3</sup>, is indicated in Table II.

TABLE II  
 $T_g$  and  $T_{50G}$  in Starch with Sorbitol

% Sorbitol	$T_{50G}$ (°C)		$T_g$ (°C)
	TEMPOL	DMAT	
0	72 ± 3	125 ± 6	90
5	75 ± 2	109 ± 8	
10	77 ± 1	122 ± 3	62
17		127 ± 7	45
26	69 ± 2	114 ± 3	32
30		113 ± 3	
40	74 <sup>a</sup>	92 <sup>a</sup>	
	50 <sup>b</sup>	60 <sup>b</sup>	
100	57	80	–25

Vapor content of samples are indicated in Table I.

<sup>a</sup> Transition of the probe–sorbitol in starch.

<sup>b</sup> Transition of the exuded probe–sorbitol.

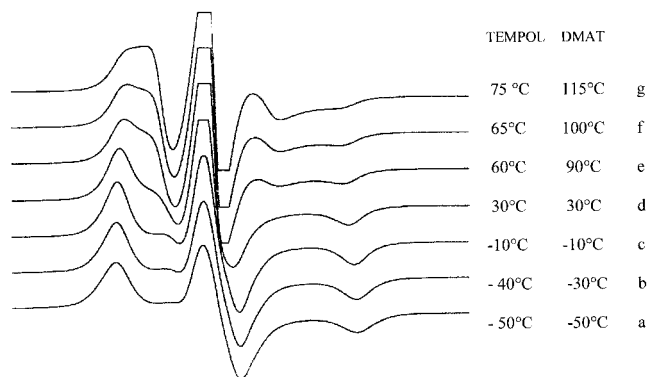


Figure 3 ESR spectra of TEMPOL and DMAT in starch at different temperatures.

### ESR investigation

ESR experiments were realized after treatment at 120°C for 10 min. In principle, the state of materials corresponds to the state measured by calorimetry on the second scan.

Behavior of spin probes in hydrated starch (13.9% water d.b.)

Figure 3 displays spectra of TEMPOL in starch at different temperatures from –50 to 75°C. Increasing the temperature results in a progressive deformation of the signal. At –50°C, one obtains the classical spectrum [spectrum (a)] of a probe strongly immobilized in the matrix [with slow rotations of  $\text{NO}^\circ$  ( $5 \cdot 10^{-9} \leq \tau_r < 10^{-7}$  s)], and a hyperfine split  $2A_{zz} = 72$  Gauss. At 75°C [spectrum (g)], the signal is more narrow ( $2A_{zz} = 62$  Gauss), which shows that the reorientation of the probe is rapid ( $5 \cdot 10^{-11} < \tau_r \leq 10^{-9}$  sec). These types of spectra are usually observed in homogeneous media, or when the probe is in a unique local environment.

Exactly the same behavior occurs with DMAT, but at considerably higher temperatures. For instance, spectrum (f) in Figure 3 is obtained at 65 and 100°C, respectively, with TEMPOL and with DMAT. When samples containing DMAT were heated at temperatures around 130°C, there was a sudden change in the shape of the spectrum, which then became identical to spectra obtained at very low temperatures. This is best illustrated in Figure 4, where  $2A'_{zz}$  is plotted versus temperature. When a sample heated above 130°C was then cooled and submitted to a second temperature cycle, there was no longer a change in the shape of the spectrum, whatever the temperature [spectra (e), (f), (g) are no longer observed]. In contrast, when the sample was not heated up to 130°C (e.g., only 120°C), the change of the spectrum shape was reversible in the temperature range studied. This shows that above 130°C, DMAT reacted with the matrix, probably by grafting the amino group on an aldehyde function. As

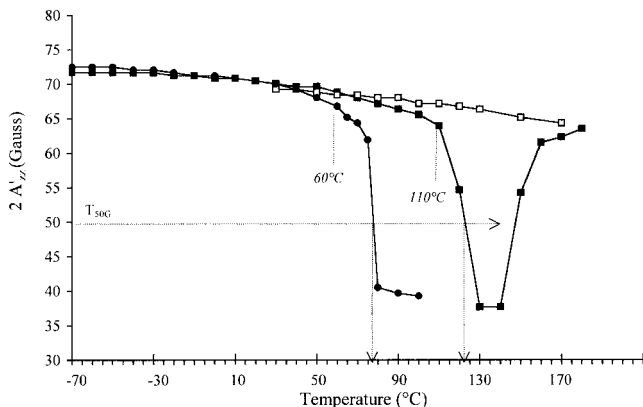


**Figure 4** Plots of extreme separation ( $2A'_{zz}$ ) versus temperature in the ESR spectra of probes in starch. Filled square, DMAT first temperature cycle; open square, DMAT second temperature cycle; filled circle, TEMPOL.

long as the temperature was kept below 130°C, the probes remained dispersed in the starch matrix.

#### Behavior of TEMPOL and DMAT in starch-sorbitol mixtures

With starch samples containing sorbitol up to 29%, the overall features of the spectra remained the same, that is, a unique local environment was observed. However, at low temperatures,  $2A'_{zz}$  depended on the percentage of sorbitol. For instance, with TEMPOL, the immobilized signal [spectrum (a) in Fig. 3] was obtained at  $-50^{\circ}\text{C}$  for 0% sorbitol, at  $-20^{\circ}\text{C}$  for 11% sorbitol, and at  $-10^{\circ}\text{C}$  for 26% sorbitol.

At 40% of sorbitol, a more complex spectrum (Fig. 5) was observed in the particular temperature of  $50^{\circ}\text{C}$ . This temperature corresponded to the rapid rotation ( $T_{50G}$ ) of TEMPOL in sorbitol. So this signal should be the superposition of the probe signals in two different media, one typical of the highly immobile molecule [lines  $H_{(+)}$ ,  $H$ ,  $H_{(-)}$ ] and the other of a free probe in sorbitol [lines  $h_{(+)}$ ,  $h$ ,  $h_{(-)}$ ]. Similar results were observed with DMAT.

#### Transition in rapid-tumbling region ( $T_{50G}$ ) and glass transition ( $T_g$ ) in starch, sorbitol, and mixtures

$T_{50G}$  values (as the temperature at which the extreme separation  $2A_{zz}$  was equal to 50 Gauss) are given for TEMPOL and DMAT in Table II. For both TEMPOL and DMAT,  $T_{50G}$  values in sorbitol were lower than in starch (especially for DMAT), showing that the probes have a higher mobility in the former matrix (sorbitol).

As it is well established in literature,  $T_{50G}$  increased with the molecular volume of the probe. However, differences observed between TEMPOL and DMAT in starch (around  $5^{\circ}\text{C}$ ) and in sorbitol (around  $20^{\circ}\text{C}$ ) are far too high to be explained only by molecular weight and volume (Fig. 1). These results suggest that DMAT

develops interactions (hydrogen bonds) with both starch and sorbitol. Such hydrogen bonds seem to restrict more the mobility of DMAT in starch than in sorbitol. TEMPOL, which is a secondary alcohol, probably interacts far less than the tertiary amino group of DMAT.

This hypothesis was supported by the behavior of TEMPOL. This probe (Fig. 1) cannot interact with starch or sorbitol. Its  $T_{50G}$  in starch ( $54^{\circ}\text{C}$ ) is lower than  $T_{50G}$  of TEMPOL and differences observed between TEMPOL and TEMPOL are smaller than those observed between TEMPOL and DMAT.

Depending on the interaction of a probe with a matrix, its  $T_{50G}$  can be expected to be either lower or higher than calorimetric  $T_g$ .<sup>13,14</sup> In hydrated starch,  $T_{50G}$  of DMAT (strong hydrogen bonding) was higher than  $T_g$ , while the opposite was observed for TEMPOL (lower hydrogen bonding tendency). In sorbitol,  $T_{50G}$  of both probes were far higher than  $T_g$ .

DSC and ESR experimental results on  $T_g$  and  $T_{50G}$  evolution with sorbitol content were not at all going in the same direction, since  $T_g$  strongly decreased with increasing sorbitol content. Surprisingly, when the percentage of sorbitol in starch increased up to 26%,  $T_{50G}$  for both DMAT and TEMPOL remained almost constant (Table II).

With DMAT, only a significant decrease of  $T_{50G}$  was observed when the content of sorbitol exceeded 29%. This clearly showed that, in this case, no correlation existed between  $T_g$  and  $T_{50G}$ . It is well known that  $T_g$  values are sensitive to plasticization.<sup>3</sup> This was not the case of  $T_{50G}$  values.

DMAT and TEMPOL can interact equally with both starch and sorbitol. The rotation of these probes in rapid-tumbling region ( $T_{50G}$ ) are more hindered in starch than in sorbitol (especially for DMAT). So, in mixtures, according to the shape of the spectrum (clas-

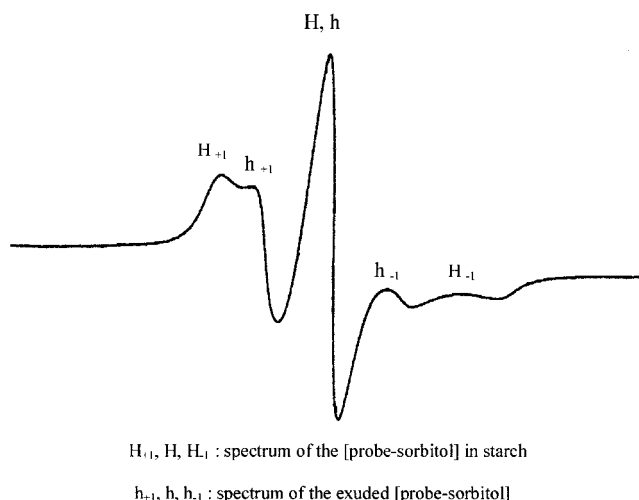


**Figure 5** TEMPOL in starch containing 40% sorbitol (spectrum recorded at  $50^{\circ}\text{C}$ ).

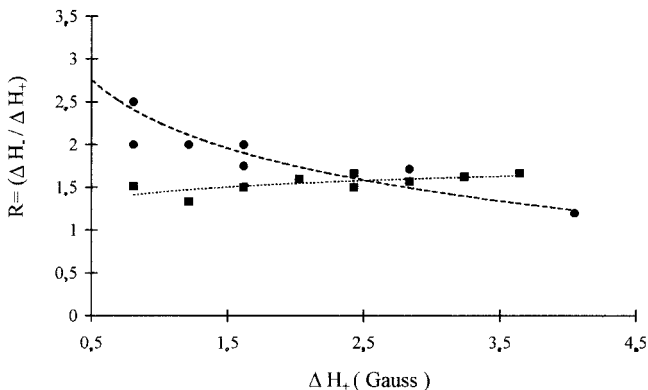


**Figure 6** Diffusion mechanism with TEMPOL (square) and DMAT (circle) in starch with or without sorbitol.

sical or complex) and  $T_{50G}$  values, we may determine if the probe is located in starch and/or in sorbitol phases.

In mixtures up to 26%, only a single environment was observed and  $T_{50G}$  were close to those of starch. So, roughly, it could be expected that probes were mainly located in this phase. However, according to this suggestion,  $T_{50G}$  like  $T_g$  values should have decreased with increasing sorbitol content; however,  $T_{50G}$  was not sensitive to the presence of sorbitol. Therefore, it seems more conceivable to admit that the transition observed in these mixtures would characterize the probe-sorbitol interaction in starch (with  $T_{50G}$  of sorbitol in starch higher than  $T_{50G}$  of pure sorbitol).

The mixture containing 40% sorbitol showed a second environment at a temperature close to that of the probes in pure sorbitol. This result together with the former likely means two sorts of sorbitol molecules: sorbitol in starch [lines  $H_{(+)}$ ; Fig. 5] and exuded sorbitol [lines  $h_{(+)}$ ; Fig. 5]. This interpretation is close to that done from calorimetry results, where the demixion of sorbitol was put in evidence for system concentrated in plasticizer.

Transitions in slow-tumbling region, starch, sorbitol, and mixtures

The mode of diffusion of the probes in the low-tumbling region was determined on the basis of the positions of the peaks at high and low fields in ESR using eq. (1);  $R$  values ranging from 1.5 to 3 reveal a Brownian rotational diffusion type, while  $R$  values below 1.5 characterize a jump-tumbling diffusion.

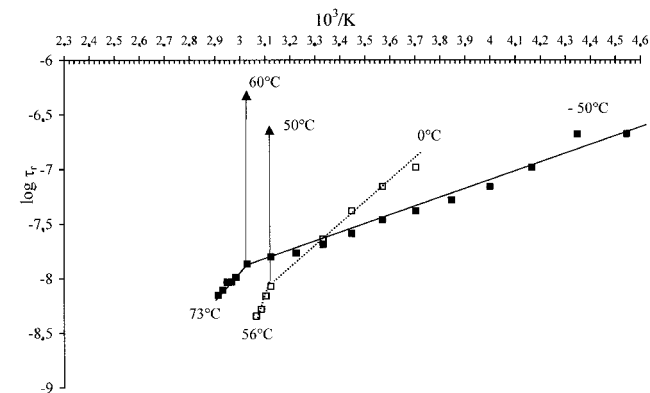
In Figure 6, we have plotted experimental  $R$  values versus  $\Delta H_+$ , which is used in the temperature range corresponding to the low-tumbling region. TEMPOL typically corresponded to a moderate jump diffusion probe, whatever the sorbitol content in starch. Similar behavior of TEMPOL has been observed in other matrices, even if they were able to form hydrogen bonds,

like butanol<sup>6</sup> and poly(ethylene terephthalate).<sup>15</sup> In contrast, DMAT displays a typical Brownian diffusion. This is usually observed for large probes, or probes strongly interacting with the matrix by hydrogen bonding. This is in agreement with the overall behavior of the two probes described here.

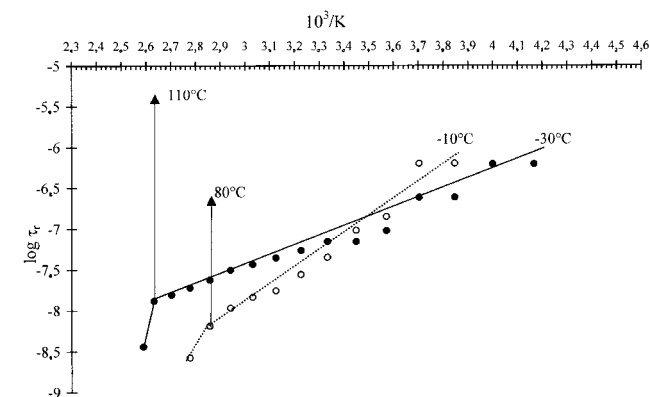
Once the diffusion model is known, the rotational correlation times ( $\tau_r$ ) can be related to temperature [eqs. (2) and (3)], which gives access to activation energies of the different transitions observed. Correlation times were calculated in the slow-tumbling region according to free diffusion (TEMPOL) and Brownian (DMAT) models.

Plots of  $\log \tau_r$  versus  $10^3 T^{-1}$  in starch and in pure sorbitol are shown in Figure 7. Both TEMPOL and DMAT revealed breaking points at, respectively, 60 and 110°C in starch, and 50 and 80°C in sorbitol. These breaking points do not correspond to transitions, but to the limit of validity of eq. (2). As it is also shown in Figure 3, at these temperatures, the type of movement is changing.

$E_a$  values of TEMPOL in both starch and sorbitol are lower than those of DMAT (Table III). Again, these results reflect the strength of hydrogen bonds.  $E_a$  values of TEMPOL and of DMAT in starch are lower than



TEMPOL (with  $\tau_r$  calculated according to free diffusion model)



DMAT (with  $\tau_r$  calculated according to brownian model)

**Figure 7**  $\tau_r$  of probes in starch (continuous line) and sorbitol (dashed line).

**TABLE III**  
Activation Energy ( $E_a \cdot \text{KJ mole}^{-1}$ ) of Probes in Starch,  
Sorbitol, and Mixtures

% Sorbitol	TEMPOL	DMAT
0	16.6 $\pm$ 1.2	21.5 $\pm$ 1.6
5	18.7 $\pm$ 1.3	26.4 $\pm$ 0.9
10	20.4 $\pm$ 0.6	29.1 $\pm$ 2.7
17		30.3 $\pm$ 3.2
26	25.6 $\pm$ 3.0	34.4 $\pm$ 2.0
30		33.0 $\pm$ 1.4
40	34.0 $\pm$ 0.6	36.5 $\pm$ 2.0
100	35.4	38.4 $\pm$ 2.0

those in sorbitol. This means that in the slow-tumbling region, probes are much more hindered in sorbitol than in starch (contrary to  $T_{50G}$ ). This result is very likely due to the differences of the structure of the matrix, sorbitol and starch (density, crystallinity, etc.). In starch containing sorbitol (Table III), there is a shift of activation energy from starch to sorbitol.  $E_a$  in mixtures increases with the percentage of sorbitol.

In the region of very slow tumbling, another difference can be noticed when the percentage of sorbitol increases. At very low temperature ( $-80^\circ\text{C}$ ), the width of the rigid spectrum is  $2A_{zz} = 72$  Gauss. At a certain temperature, change of the spectrum shape can be observed. It corresponds to a start of probe mobility, which was immobilized in the frozen matrix (this is shown in Fig. 8 by marks A–E). Figure 9 shows that the temperature of probe mobility start measured by ESR increases with percentage of sorbitol in the system. There is a correspondence with temperature change of a low-temperature relaxation, previously evidenced by dynamic mechanical thermal analysis (DMTA)<sup>13</sup> and reported in the figure. In the slow-tumbling region, probe mobility is dependant on hole volumes in which they are moving. Hole volume seems to decrease with increase of sorbitol content.

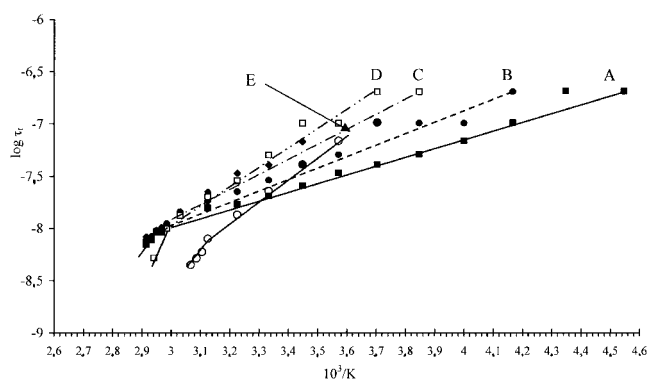


**Figure 8**  $\tau_r$  of TEMPOL in starch with sorbitol: (filled square) 0% sorbitol; (filled circle) 6% sorbitol; (filled diamond) 11% sorbitol; (open square) 26% sorbitol; (open circle) 100% sorbitol.

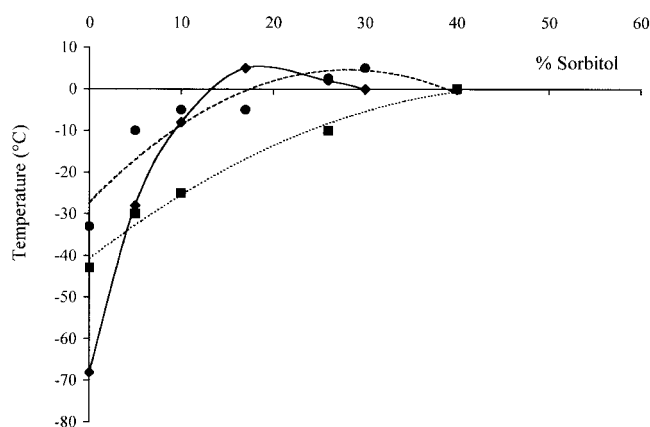


**Figure 9** Correspondence in mobility changes measured by DMTA (diamond) and ESR (circle, DMAT; square, TEMPOL) in slow-tumbling region.

#### Probes mobility at ambient temperature

Figure 10 shows variation of rotational correlation time  $\tau_r$  of probes in starch with sorbitol at constant temperature ( $30^\circ\text{C}$ ).  $\tau_r$  increases with sorbitol content (moderately for TEMPOL, strongly for DMAT), then reaches the maximum around 40% of sorbitol. These results could be related to a previous study which showed that sorbitol leads to a reduction of oxygen permeability in glassy starch films.<sup>2</sup> This correlation suggests that diffusion properties are linked to local mobility in a glassy system. But caution has to be taken with this correlation because the important difference between molecular weight of probes and oxygen.

## CONCLUSIONS

Molecular mobility in starch sorbitol materials has been investigated by electronic spin resonance using TEMPOL and DMAT probes. Results on phase transitions in starch containing sorbitol were in agreement with the preferential complexation of probes with sor-

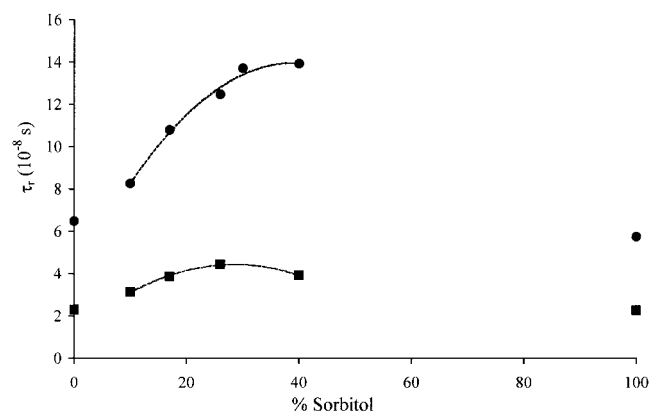


**Figure 10**  $\tau_r$  of probes DMAT (circle) and TEMPOL (square) in starch with sorbitol at room temperature.

bitol. This study also shows that low-temperature relaxations corresponding to local molecular mobility was detected.

At ambient temperature, mobility of probes inside the starch matrix are hindered by sorbitol presence. This behavior could be linked to diffusional properties, in particular oxygen permeability.

The authors thank Joelle Davy for technical assistance.

## References

1. Moates, G. K.; Noel, T. R.; Parker, R.; Ring, S. G. *Carbohydr Polym* 2001, 44, 247.
2. Gaudin, S.; Lourdin, D.; Forssell, P.; Colonna, P. *Carbohydr Polym* 2000, 43, 33.
3. Lourdin, D.; Coignard, L.; Bizot, H.; Colonna, P. *Polymer* 1997, 38, 5401.
4. Hamdani, M.; Scholler, D.; Bouquand, J.; Feigenbaum, A. *Tetrahedron* 1996, 52, 605.
5. Berliner, L. In *Spin Labelling: Theory and Applications*; Horecker, B., Kaplan, N., Marmur, J., Scheraga, H., Eds.; Academic Press: London, UK, 1976; Vol. 1, Ch. 1.
6. Kuznetsov, A. N.; Ebert, B. *Chem Phys Lett* 1974, 25, 342.
7. Freed, J. H. In *Spin Labelling: Theory and Applications*; Horecker, B., Kaplan, N., Marmur, J., Scheraga, H., Eds.; Academic Press: London, UK, 1976; Vol. 1, Ch. 3.
8. Hodge, I. M. *J Noncryst Solids* 1994, 169, 211.
9. Hutchinson, J. M. *Prog Polym Sci* 1995, 20, 703.
10. Bizot, H.; LeBail, P.; Leroux, B.; Davy, J.; Roger, P.; Buleon, A. *Carbohydr Polym* 1997, 32, 33.
11. Siniti, M.; Jabrane, S.; L  toff  , J. M. *Thermochimica Acta* 1999, 325, 171.
12. Gaudin, S.; Lourdin, D.; Le Botlan, D.; Ilari, J. L.; Colonna, P. *J Cereal Sci* 1999, 29, 273.
13. Tormala, P. *J Macromol Sci Rev Macromol Chem* 1979, 2, 297.
14. Cameron, G. G. *Comprehensive Polymer Science: Polymer Characterisation*; Pergamon Press: Oxford, UK, 1989; Vol. 1.
15. Doolan, J. G. *Polym Fibres Sci* 1992, 9, 115.